

Josephson Junction Arrays as a Variable Inductor in RF Circuits and Tunable Filters

V. Kaplunenko and Gerd M. Fischer

STI Conductus, 969 West Maude Avenue, Sunnyvale, CA 94085 USA

Abstract. We report on the investigation of the effects of the nonlinear inductance of huge Josephson junction arrays on high-quality RF circuits. The inductance of a single junction is far too small for use in many RF applications; however, Josephson junction stacks and especially intrinsic Josephson junctions in crystalline-layered superconductors open new opportunities. The stack inductance can be altered by changing a DC Josephson current either using an external bias current or an external magnetic field applied to a closed superconducting loop containing two stacks connected in parallel. Using stacks of Josephson junctions in the LC resonators, a tunable 4-pole, 15 MHz band-pass filter with a center frequency at 1.1 GHz was designed. The filter was simulated in the time domain and the response was converted to the frequency domain. It was found that using an input power level of -62 dBm, corresponding to 0.5% of the junctions' critical current, a linear approximation for the stack nonlinear inductance can be used. By changing the applied magnetic field, a tuning range of 20% was demonstrated with a tuning speed of 2 μ s or better. An estimate of the losses is also given. In addition, power handling up to -26 dBm is reported using increasing circuit complexity.

1. Introduction

It is well known that an individual Josephson junction exhibits an inductance of about 0.2 pH, which is far too small for many practical RF circuit applications. Fortunately, there are the opportunities of either using artificially-engineered Josephson junction stacks containing hundreds of junctions [1] or intrinsic Josephson junction stacks with tens of thousands of junctions already present in crystalline layered superconductors like $\text{Bi}_2\text{Sr}_2\text{CaCu}_2\text{O}_8$ (BSCCO), $(\text{Bi}_{1-x}\text{Pb}_x)_2\text{Sr}_2\text{CaCu}_2\text{O}_8$ $(\text{Bi}_{1-x}\text{Pb}_x)_2\text{Sr}_2\text{Ca}_2\text{Cu}_3\text{O}_{10}$, $\text{Tl}_2\text{Ba}_2\text{Ca}_2\text{Cu}_3\text{O}_{10}$ (TBCCO), $\text{Tl}_2\text{Ba}_2\text{Cu}_1\text{O}_6$, or $\text{Pr}_{2-x}\text{Ce}_x\text{CuO}_4$. The crystalline structure of the latter materials is a set of superconducting planes separated by layers of insulators, which form unshunted Josephson junctions [2]. As a result, the inductance of such a system can be a few thousand times that of a single junction (about few nHs.) This leads to a new class of non-linear dynamic effects, which can be employed in RF circuits. We consider a case when a small RF current (compared to the critical current of the junctions) is applied to the stack. In this case we can use differential inductance of the junction:

$$L = \Phi_0 / \sqrt{I_c^2 - I^2}, \quad (1)$$

where Φ_0 is the flux quantum, I is the dc bias current, and I_c is the critical current of the junction [3]. An N -junction array will have N times larger inductance, making it suitable for RF applications for high enough N .

The choice of a superconducting band-pass filter as the circuit to be investigated was straightforward. The filters are very sensitive to small variations of their elements, they easily can be measured, and they are being used in commercial telecommunication systems. All practical systems have to be trimmed to meet frequency specifications, and there is a desire for tunable systems with larger tuning range. Currently, either superconducting tuning tips (inductance variation) or dielectric tuning tips (capacitors variation) are mechanically positioned above a particular thin-film resonator in order to change its center frequency [4]. Using the variable inductance of Josephson junction stacks instead of microstrip in filter resonators seems very attractive [5]. With the stack of Josephson junctions always in the superconducting state, the insertion loss is expected to be small. The inductance can be tuned by applying an external magnetic field, thus no leads and moving parts are required to tune the filter. The millions of junctions in the stacks made from layered superconductors that are required for one resonator will occupy less than two-by-two millimeters, comparable to or less than the size of the present inductances in commercial HTS filters.

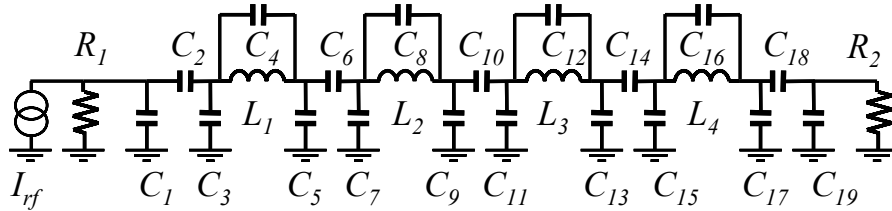


Figure 1. Equivalent circuit of the 4-pole, 15 MHz band-pass fixed frequency filter with center frequency 1.1 GHz. $L_1 = L_2 = L_3 = L_4 = 4124$ pH, $C_1 = C_{19} = 1.8782$ pF, $C_2 = C_{18} = 1.18397$ pF, $C_3 = C_{17} = 5.12467$ pF, $C_4 = C_8 = C_{12} = C_{16} = 2.0493$ pF, $C_5 = C_7 = C_{13} = C_{15} = 5.854$ pF, $C_6 = C_{14} = 0.18187$ pF, $C_9 = C_{11} = 5.94$ pF, $C_{10} = 0.139$ pF, $R_1 = R_2 = 50 \Omega$.

Figure 1 shows the lumped element model of a 4-pole Chebyshev filter with capacitively-loaded inductors in the resonators [6]. This circuit was used as a starting point for the simulations, where subsequently the inductances were substituted by arrays of Josephson junctions. The self-capacitance of the Josephson junctions in the array contributes a capacitance to be added to the capacitors $C_{4,8,12,16}$ in Figure 1. In the simulation, an ideal RF current source I_{rf} with infinite impedance was used and the circuit is terminated with 50Ω resistors at the input and the output.

2. Numerical methods

2.1 Identical Josephson junctions array approximation

In the simple RSJ model, a single unshunted Josephson tunnel junction can be represented by three elements: a capacitor (typical value about 0.1 pF), a shunt resistor representing the sub-gap resistance R_j (about 30 to 100 Ω for high-quality junctions), and the Josephson element with a critical current I_c (usually below 1 mA). The latter is tied to the quantum mechanical phase difference φ , and the bias current I_b across it by:

$$I_b = I_c \sin(\varphi) \quad (2)$$

To simulate a series array of N identical junctions we were using a single element with N times larger resistance, and N times smaller capacitance compared to a single junction. The Josephson array element now can be described as:

$$I_b = I_c \sin(\varphi / N) \quad (3)$$

Indeed, the phase difference across the array produced by the bias current I_b can be found from (3):

$$\varphi = N \bullet \arcsin(I_b / I_c) = N\varphi_1, \quad (4)$$

where φ_1 is the phase across a single junction in the array. Using the Josephson array element approximation boosted the speed of the simulations by about two orders of magnitude.

2.2 Obtaining S-parameters from time-domain simulations

Since the frequency-domain analysis of the filter with the non-linear inductances is a rather complex task, we have decided to run the numerical simulation using the time domain. This relatively quickly enables us to find the operational margins of such a complex device. To define the S-parameters of the filter, an ideal single tone current source (I_{rf} in Figure 1 or its complex equivalent i_{rf} in the following discussion) was used. For each frequency the instantaneous voltages V_1 and V_2 across the active loads (R_1 and R_2) were collected. A Hilbert transform was used to retrieve the envelope amplitudes and phase of the complex voltages v_1 and v_2 from V_1 and V_2 correspondingly. Their envelope amplitudes; V_1^a , V_2^a ; and the phase, V_1^φ (taken relative to the phase of i_{rf}) were recorded over the simulation time. This time was chosen as needed to obtain stable data. The S-parameters S_{21} and S_{11} [7] can be calculated as (I_{rf}^a is amplitude of i_{rf}):

$$\begin{aligned} |S_{11}| &= \left| \frac{v_1 / (i_{rf} - v_1 / R_1) - R_1}{v_1 / (i_{rf} - v_1 / R_1) + R_1} \right| = |2v_1 / R_1 i_{rf} - 1| \\ &= \sqrt{(2V_1^a / R_1 I_{rf}^a)^2 - 4(V_1^a / R_1 I_{rf}^a) \cos(V_1^\varphi) + 1} \end{aligned} \quad (5)$$

$$|S_{21}| = \left| \frac{2v_2}{v_1 + R_1(i_{rf} - v_1 / R_1)} \right| = \frac{2V_2^a}{R_1 I_{rf}^a} \quad (6)$$

First, the circuit in Figure 1 was tested in the time domain using the modified WinS schematic editor and simulator [8], then the S-parameters were obtained as described above (see equations (5)-(6)). The result was exactly the same as the curves obtained independently in frequency-domain simulations using different standard simulation tools. This proves the validity of the concept of time-domain simulations, and permits us to investigate non-linear systems using this approach.

Since the ideal current source equally distributes current between the two ports (R_1 and R_2), the input RMS power P_{in} incident on the filter input is calculated as follows:

$$P_{in} = (I_{rf}^a / 2)^2 R_1 / 2 \quad (7)$$

3. Tunable Filter

3.1 Inductance non-linearity compensation

The RF current causes an unwanted instantaneous inductance variation of the Josephson junction stack. If this variation is negligible we have the fixed-frequency filter as in Figure 1. To minimize that inductance variation we try to use two identical arrays, which can be connected either in series (Figure 2b) or in parallel (Figure 2c) with respect to the

RF current path. The inductors L (Figure 2b) have a very high inductance compared to the array inductance and serve to create a DC bias in response to the external magnetic field. The inductors are located on the opposite sides of each array to provide opposite DC bias current directions in response to the field. For both configurations (see arrows in Figure 2b-c) the external magnetic field creates DC currents that are parallel to the RF current in one stack and antiparallel in the other. An increase in the magnetic field will increase both stack inductors. For a nonzero DC bias current, the net current is always increasing through the one stack and decreasing through the other one by the RF current, depending on the DC current direction. This will result in a difference in the inductances of the two stacks, δL . Figure 2d shows the maximum inductance variation δL caused by the RF current δI of amplitude 0.01 mA as a function of the bias DC current magnitude created by the magnetic field for the series (curve 1) and the parallel configuration (curve 2). The inset shows δL as a function of the RF current for a constant DC bias current of 0.5 mA. The parallel configuration (curves 2) offers smaller inductance non-linearity at higher biases, and thus it was selected for the more detailed investigation. Note that the inductance variation of a single array (without inductance compensation) would appear in Figure 2d as an almost vertical line.

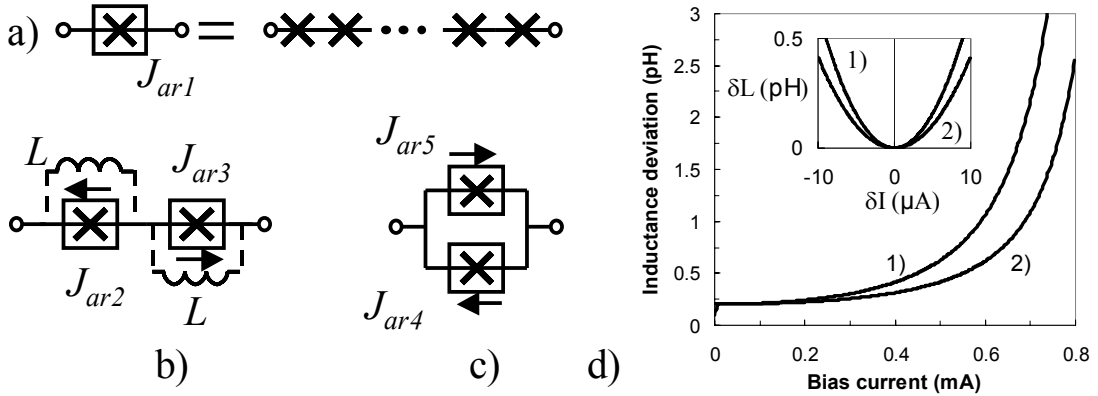


Figure 2. (a) Squared cross J_{ar1} denotes the array of identical Josephson junctions with critical current 1 mA. Series (b), and parallel (c) configuration of arrays. d) Maximum inductance variation δL (see insert on d)) caused by RF current δI of amplitude 0.01 mA as function of DC bias current created by magnetic field for the serial (curves 1) and parallel configurations (curves 2). J_{ar2} , J_{ar3} each consist of 6150 junctions, and J_{ar4} , J_{ar5} each consist of 24600 junctions, resulting in the same inductance of 4052.2 pH at zero magnetic field for both configurations. The inset in d) shows the instantaneous inductance change as a function of RF current at a constant DC bias of 0.5 mA.

3.2 Tuning range

By replacing inductances in Figure 1 with the stacks of junctions in the parallel configuration (Figure 2c) the circuit under test was built and simulated for different DC bias currents. Then the S-parameters for the tunable 4-pole filter were calculated using equations (5)-(6). The number of junctions in each array was selected to have an inductance value slightly smaller for the fixed-frequency circuit (Figure 1), because the DC bias current will always increase the inductance of an array. This was done to minimize the deviation from the optimum values for the resonator impedance as well as the resonator coupling over the whole tuning range. Figure 3 shows the S-parameters S_{21} and S_{11} over the frequency range from about 850 MHz up to about 1.15 GHz. The tuning

range shown is about 20%. Obviously the acceptable maximum tuning range depends on the application specifications with respect to the return loss, the insertion loss and the acceptable bandwidth change. As can be seen in Figure 3 S_{11} is slightly degraded at the very high and very low frequencies because of the impedance mismatch due to the resonators detuning from the optimal frequency. The bandwidth also decreases from high to low frequency because of a decrease of the interconnect capacitors coupling (see $C_{2,6,10,14,18}$ in Figure 1.)

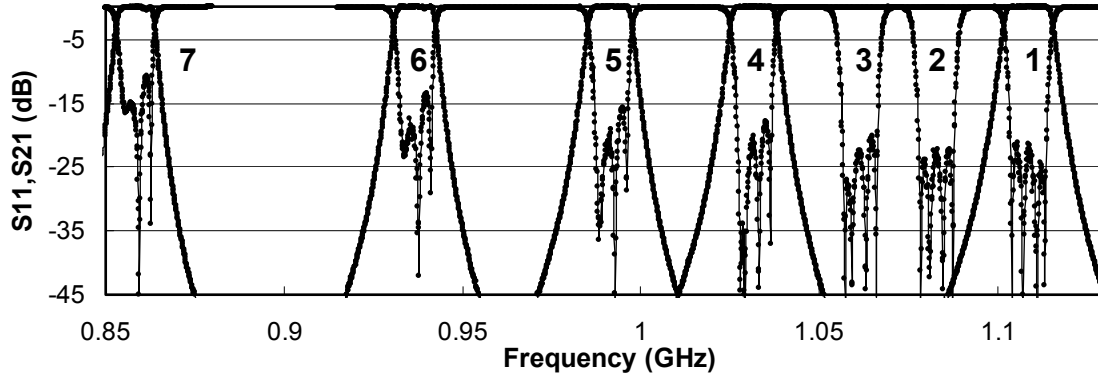


Figure 3. S-parameters of the tunable band pass filter at different bias currents I_b , obtained for parallel inductance configuration (see **Figure 2c**), and no losses. I_b was set to 0.0 mA (1), 0.3 mA (2), 0.4 mA (3), 0.5 mA (4), 0.6 mA (5), 0.7 mA (6), 0.8 mA (7). For clarity the S_{21} parameters are not shown for curves 2 and 3. Input power -62 dBm.

3.3 Input power handling capability

The low input power level of -62 dBm in Figure 3 was selected mainly to avoid a large frequency shift to lower frequencies associated with the power increase. The shift obtained at constant DC bias of 0.3 mA and being taken relative to the -68 dBm input power level was about 0.2 MHz at input power -62 dBm; 1.1 MHz at -56 dBm, and 2.3 MHz at -52.5 dBm. This is correlated to the third-order intercept point $IP3 = -42$ dBm obtained at the same bias, and the 1 dB compression point of -46 dBm. An additional ideal AC current source was added to the resistor R_I in Figure 1 to generate the third-order IM frequencies for $IP3$ simulations. The input power of -62 dBm is far too small for any practical applications, but by increasing the circuit complexity it can be increased to realistic values (see further discussion below.)

3.4 Losses

The main source of losses when using Josephson junctions will be the shunting sub-gap resistance R_j of the individual junction, which gives rise to a leakage current. Higher quality junctions have higher R_j . Our simulations have shown that adding a $50N \Omega$ shunt resistor to the Josephson junction equivalent circuit in the array ($50N \Omega$, where N -number of average quality junctions in array) causes a transmission loss about 0.1 dB. Using high quality junctions arrays with shunt resistance of $100N \Omega$ (100Ω per junction) reduces the transmission loss to the level well below the simulations accuracy of 0.02 dB.

Another source of losses will be discussed in the next paragraph, when more than two arrays of junctions will be connected in parallel for better power handling. This requires the addition of a normal-metal resistor R_b to be connected in series with the inductors (Figure 4) in order to break the additional superconducting loop. The following transmission losses were obtained for this small resistor added to all resonators built from

two arrays of junctions: 0.02 Ω : 0.65 dB, 0.01 Ω : 0.4 dB, 0.05 Ω : 0.17 dB, 0.002 Ω : 0.1 dB, 0.001 Ω : below simulations accuracy.

3.5 Possible ways to improve power handling

From equation (1) it is relatively easy to find that the relative small inductance change $\Delta L/L$ depends only on relative bias current change $\Delta I_c/I_c$. Thus increasing critical current of the junctions and proportional increase of the number of the junctions in all arrays can improve input power handling capability. Unfortunately this works well only for small critical currents. The equation (1) is correct only for the case of uniform current distribution within the junction area. To maintain this requirement the junction dimensions must be less than four times the Josephson penetration depth, λ_j . Thus providing the critical current density J_c the maximum critical current I_c^{max} can be estimated as:

$$I_c^{max} = 16J_c\lambda_j^2 = 16J_c(\Phi_0/2\pi J_c\mu_0 t) = 8\Phi_0/\pi\mu_0 t, \quad (8)$$

where t is the magnetic gap between superconducting plates forming tunnel Josephson junction (it equals to the thickness of insulator layer plus two London penetration depths). For most technologies it is very difficult to make junctions with $I_c^{max} > 1$ mA.

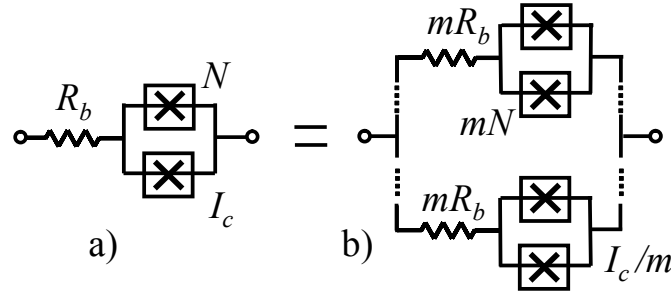


Figure 4. a) Two Josephson junction arrays built from N junctions of critical current I_c and break resistor R_b are equivalent to m pairs of arrays consisting of mN junctions of critical current I_c/m each, and break resistor mR_b (b).

Fortunately, there is an opportunity to overcome this problem. Figure 4a shows the parallel array structure we were using to simulate the tunable filter plus the additional small break resistor R_b . As mentioned in section 3.4 adding such a small resistor does not change the filter properties, but it allows the electrically equivalent circuit shown in Figure 4b to be built. Break resistors are needed to deliver the external magnetic field to all pairs of arrays. Their values should be small as possible because they only serve to break the superconducting loop. Circuit b) offers two advantages. The first one is the rest on R_b requirement to be small. For numbers of pairs $m = 64$, it can be only 0.064 Ω (see section 3.4), which is reasonable value for gold-to-HTS materials interface. The second one is that the use of 1.0 mA critical current junctions in configuration b) equivalent to 32.0 mA critical current junctions in configuration a). Thus the power handling capability can be increased by 36 dB to the level of -26 dBm (see Figure 3), which is comparable to the level provided by commercial non-tunable HTS filters. The cost of this is the increase of the total number of junctions by factor of m^2 .

To demonstrate this approach we have simulated a filter with $m = 4$, and $m = 8$ number of stack pairs using same resonator parameters as for circuit simulated in Figure 3. Figure 5a shows the simulation of the 1 dB compression point, and Figure 5b the simulation of the IP3 for a circuit with $m = 1$ (see also results in Figure 3) and for a circuit with $m = 4$ (a), and $m = 8$ (b). Figure 5 shows the increase of the 1 dB compression point by 12 dB according to the expected power handling capability

increase, and IP3 is increased by 13 dB, which is within the error caused by the FFT procedure [9]. The 1 dB compression point simulation is more accurate, because it uses a single tone excitation signal, and thus the FFT is taken over a time of an integer multiple of the tone period.

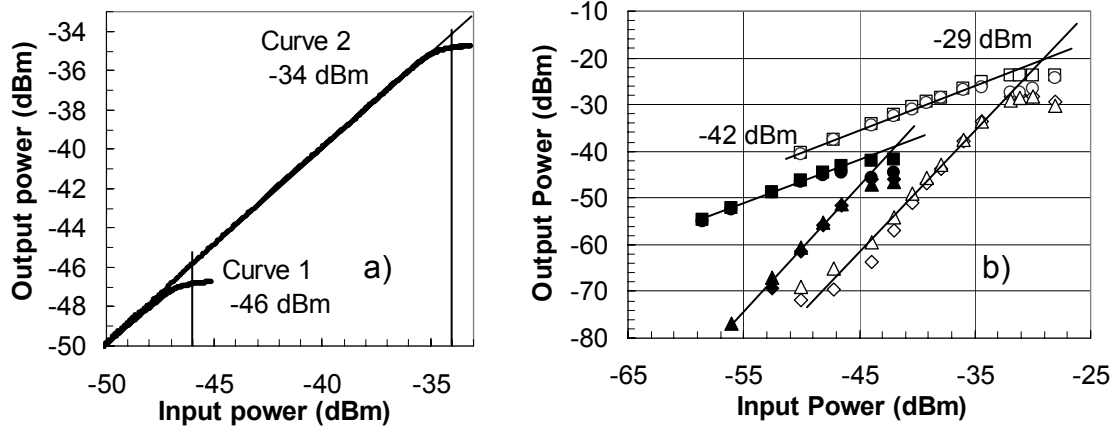


Figure 5. a) 1 dB compression point simulated for resonator with one pair of Josephson stacks (curve 1), and for one with four pairs (curve 2). b) Third-order intercept point (IP3) obtained for resonator with one stack pair resonator (filled marks, IP3 = -42 dBm), and eight stacks resonator (open marks, IP3 = -29 dBm). Triangle and diamond marks denote third-order slope, while square and circle marks denote fundamental slope.

4. Discussion and Conclusion

To implement a filter with the tuning range as in Figure 3 and an input power handling capability of -26 dBm one needs to lay out 100,761,600 junctions for each resonator. The only way to provide that many junctions is to use the intrinsic Josephson junction stacks in layered superconductors. The critical current of 1 mA is an achievable value (see, for instance, the measurements of a single junction fabricated using stack technology in [10]). The most accurate measurement of the sub-gap resistance of a stack of 10 junctions was obtained from intrinsic tunneling spectroscopy, with a value of more than 100Ω at temperatures around 70 K [11]. The stack size containing the above-mentioned number of junctions divided by 128 (the actual number of arrays in one resonator) would be only about 1.5 mm. This size may be reduced by using arrays of Josephson junction stacks as was demonstrated in [12], where a 256-stack array containing over 10,000 junctions were fabricated. For RF filter applications it is important that a superconducting connection of these stacks is achieved. For many applications the stack size is limited by the effect of gap suppression caused by quasiparticle injection and heat. This may not be the case for the filter application since the stack will be operating in the superconducting mode and will only be loaded with a small amount of power.

There are a few applications that require only a 2% tuning range, which reduces the number of junctions by a factor of 10. This can be implemented by replacing only a fraction of the inductances in Figure 1 with the Josephson junction stacks. Thus, only 10,076,160 junctions per resonator are needed to build such a circuit with 78,720 junctions in each stack.

The best approach to deliver magnetic field to the individual resonator is the superconducting flux transformer. It can be made either from a superconducting wire or

a superconducting thin film on a separate chip, which can be flipped onto the filter substrate. Using this method, the source of the external magnetic field, a normal coil coupled to the opposite end to the transformer, can be moved away from the tightly packed chip area. Thus the magnetic field source and the superconducting filter can be completely RF decoupled by the transformer. Even the metallic wall of the filter package can be in between input turn of transformer and the normal coil.

Since the basic limitations of using arrays of Josephson junctions for filter tuning are understood from time-domain simulations, the design of an actual filter can be made using standard tools based on frequency-domain simulations. Within these limits the junction inductance is well described by equation (1), and can be used as a linear element.

To avoid losses in the tunable filter, all Josephson junctions must have a critical current value large enough to prohibit them from switching to the normal state, though junction uniformity is insignificant in comparison to other Josephson junction applications. Thus, to build tunable filters containing millions of Josephson junctions requires the development of a new kind of *Intrinsic HTS engineering* as fabrication technology.

Acknowledgement

We would like to thank Nick Maltsev for help in the selection of the appropriate mathematical approaches. The assistance of the STI/Conductus RF team, namely S. Berkowitz, K. Dustakar, G. Tsuzuki, and S. Ye is highly appreciated.

References

- [1] S. J. Berkowitz, C. F. Shih, W. H. Mallison, D. Zhang, A.S. Hirahara 1997 Demonstration of a 20 GHz phase shifter using high-temperature superconducting SNS junctions IEEE transaction on Applied Superconductivity 7 3056-3059
- [2] A. A. Yurgens 2000 Intrinsic Josephson junctions: recent developments Supercond. Sci. Technol. 13 R85-R100
- [3] K. K. Likharev 1986 Dynamics of Josephson junctions and circuits (Gordon and Breach science publishers, New York)
- [4] US Pat. 6,347,237 and US Pat. referenced therein
- [5] V. Kaplunenko, and G Fischer 2002 STI Conductus Inc. Internal patent application
- [6] D. Zhang, Guo-Chun Liang, Chien-Fu Shih, M. E. Johansson, and R. S. Withers 1995 Narrowband Lumped-Element Microstrip Filters Using Capacitively-Loaded Inductors IEEE Trans. On Microwave Theory and Techniques 43 3030-3036
- [7] Hewlett Packard, Test & Measurement Application Note 95-1
- [8] V. Kaplunenko Superconducting circuit editor and simulator <http://www.rsfq.net>
- [9] W. H. Press, S. A. Teukolsky, W. T. Vettering, and B. P. Flannery 2002 Numerical recipes in C (Cambridge University Press)
- [10] A. Yurgens, D. Winkler, N. V. Zavaritsky, T. Claeson 1996 Strong temperature dependence of the c-axis gap parameter of $\text{Bi}_2\text{Sr}_2\text{CaCu}_2\text{O}_{8+x}$ intrinsic Josephson junctions Phys. Rev. B 53 R8887-88890
- [11] V. M. Krasnov, A. Yurgens, D. Winkler, P. Delsing, and T. Claeson Evidence for coexistence of the superconducting gap and the pseudogap in Bi-2212 from intrinsic tunneling spectroscopy 2000 Phys. Rev. Lett. 84 5860-5863
- [12] H. B. Wang, K. Maeda, J. Chen, P. H. Wu, and T. Yamashita 2002 Three-dimensional array of intrinsic Josephson junctions in $\text{Bi}_2\text{Sr}_2\text{CaCu}_2\text{O}_{8+x}$ single crystals Physica C 372- 376 327-330